

Coevolution of the Mammalian Middle Ear and Neocortex

Timothy Rowe

Phylogenetic analysis with x-ray computed tomography of fossilized and recent crania implicates differential growth of the neocortex in the evolution and development of the mammalian middle ear. In pre-mammalian tetrapods, the middle ear evolved as a chain of bones attached to the mandible and cranium, but in adult mammals the chain is detached from the mandible and lies behind it. The neocortex evolved concurrently with detachment of the chain. In mammalian development the auditory chain arises connected to the mandible but later detaches, recapitulating the phylogenetic transformation. In modern didelphid development, the auditory chain reaches mature size by the third week after birth and is then separated from the jaw and displaced caudally as the neocortex grows for another 9 weeks.

The mammalian middle ear contains a chain of tiny ossicles whose parallel histories in ontogeny and phylogeny are among the most famous in comparative biology (1, 2). The middle ear arose in pre-mammalian history (1–6) as an integrated component of the mandible, where it participated in a continuous arcade of bones

extending from the mandibular symphysis to the fenestra vestibuli (FV) of the inner ear (Fig. 1). The craniomandibular joint (CMJ) was formed by the quadrate and articular, which served the dual functions of hearing and feeding. Over a 100-million-year span of pre-mammalian history, the middle ear ossicles were gradually reduced, reflecting specialization for increasingly high-frequency hearing (3), while the dentary correspondingly enlarged to

undertake a greater role in feeding (4). Hearing and feeding were structurally linked in pre-mammalian history, but in mammals (5) these functions became decoupled as the auditory chain detached from the mandible and repositioned behind it. The dentary remains as the only bone in the mammalian lower jaw, articulating with the squamosal to form a new CMJ. Anatomical relations of the ear ossicles to one another and auditory function were little affected in this transformation (3). Separation of the ossicles from the mandible is common to all adult mammals and was widely regarded as the definitive mammalian character under Linnean taxonomy (6).

In modern didelphid (marsupial) development (7), as in mammals generally (1, 2, 5), the auditory chain differentiates and begins growth attached to the mandible, forming an arcade of cartilages from the FV to the mandibular symphysis (Fig. 2A). Three cartilages are present at birth. The stapes extends from the FV to the incus (quadrate), which is braced against the ventral edge of the otic capsule and articulates with the rear extremity of Meckel's cartilage. In the second developmental week, Meckel's cartilage cleaves to form the malleus (articular). The two pieces

Department of Geological Sciences and Vertebrate Paleontology Laboratory, University of Texas, Austin, TX 78712, USA.

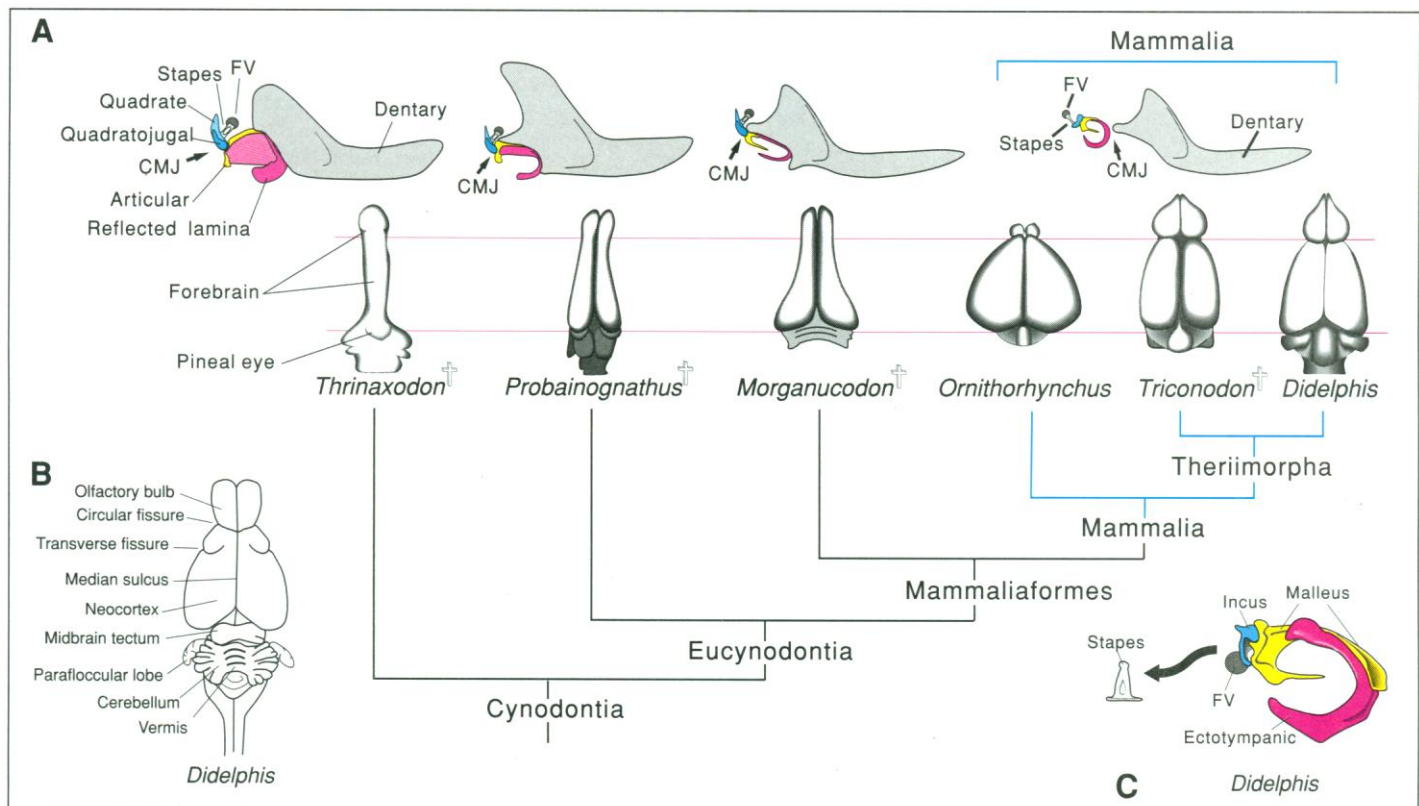


Fig. 1. (A) Coevolution of the mammalian mandible and middle ear (right lateral view) and the brain (illustrated by dorsal views of endocasts), plotted on a phylogeny of selected mammals and their closest extinct relatives (5, 19). (B) Dorsal view of the brain of *Didelphis* (opossum). (C) Right lateral

view of auditory chain of *Didelphis*; the stapes is rotated and offset from between the incus and fenestra vestibuli. Abbreviations: CMJ, craniomandibular joint; FV, fenestra vestibuli of the inner ear. Crosses signify extinct species.

then separate as Meckel's cartilage degenerates during ossification of the dentary. The dentary and ectotympanic bone (angular) begin to ossify in a common membrane and soon grow into contact with one another. Connective tissues joining them are torn at the end of the third week after birth as the entire auditory chain (stapes, incus, malleus, and ectotympanic bone) is carried backward during the next 9 weeks to its adult position behind the CMJ. Ontogeny thus recapitulates phylogeny in detachment and relocation of the auditory chain.

Two hypotheses attempt to explain the

detachment of the auditory chain from the jaw. An evolutionary hypothesis (3) views pre-mammalian history as shaped by selection for high-frequency hearing, with detachment of the chain from the mandible an extension of this trend. A developmental hypothesis (8) argues that the onset of jaw muscle functionality tears the auditory chain from the jaw. Neither hypothesis addresses both the developmental and phylogenetic transformations nor explains repositioning of the auditory chain to its new location behind the CMJ.

Using three-dimensional endocranial im-

aging (Fig. 3) with high-resolution x-ray computed tomographic scanning (9) for phylogenetic analysis of mammals and their extinct relatives, I have identified additional bony mammalian synapomorphies that arose concurrently with the repositioned auditory chain (2). Their common location about the endocranial cavity implicates the brain as a dominant morphogenic influence in mammalian cranial evolution (2, 5). Late Permian cynodonts are the first members of the mammalian "stem" lineage in which the brain filled the endocranial cavity. They have a simple tubular forebrain, with broad midbrain exposure dorsally and a pineal eye. Successive episodes of evolutionary forebrain enlargement are recorded in endocasts of *Probainognathus* (Middle Triassic) and *Siniconodon* and *Morganucodon* (Early Jurassic). A still greater relative increase in forebrain volume occurred in the last common ancestor of extant mammals (5).

This additional brain volume marks an episode of heterochrony (peramorphosis) (10) in which the mammalian brain began to grow for a greater portion of ontogeny, and probably also more rapidly, than in *Morganucodon* and more distant outgroups. Details of endocast morphology indicate that this period also marks the origin of the mammalian neocortex (2). The developing mammalian forebrain hypertrophies into inflated hemispherical cortical lobes that swell backward over the midbrain and forward around the bases of the olfactory bulbs, which are themselves inflated. The circular fissure develops between the olfactory bulb and neocortex and is visible for the first time in a Late Jurassic endocast of *Triconodon mordax* (11). The cortical hemispheres differentiate into separate neocortex (isocortex) and pyriform cortex. Each hemisphere has a columnar organization of six radial layers that are generated in ontogeny by waves of migrating cells that originate from the ventricular zone and move radially outward to achieve their adult positions (12). This inside-out pattern of neural growth is unique to mammals and produces a huge cortical volume (13). The cerebellum is also inflated and deeply folded.

The key to understanding the developmental transformation of the auditory chain is its differential growth with respect to the brain and the skull in general. Using the mandible of didelphids as an illustration, the tympanic ring or ectotympanic bone (reflected lamina of the angular) has begun to ossify at birth and at first grows more rapidly (positive allometry) than the dentary (Fig. 4). However, growth slows (negative allometry) as adult size is reached late in the third week after birth, and shortly thereafter the entire auditory chain is pulled free of the dentary. The brain continues to grow at a linear rate through a

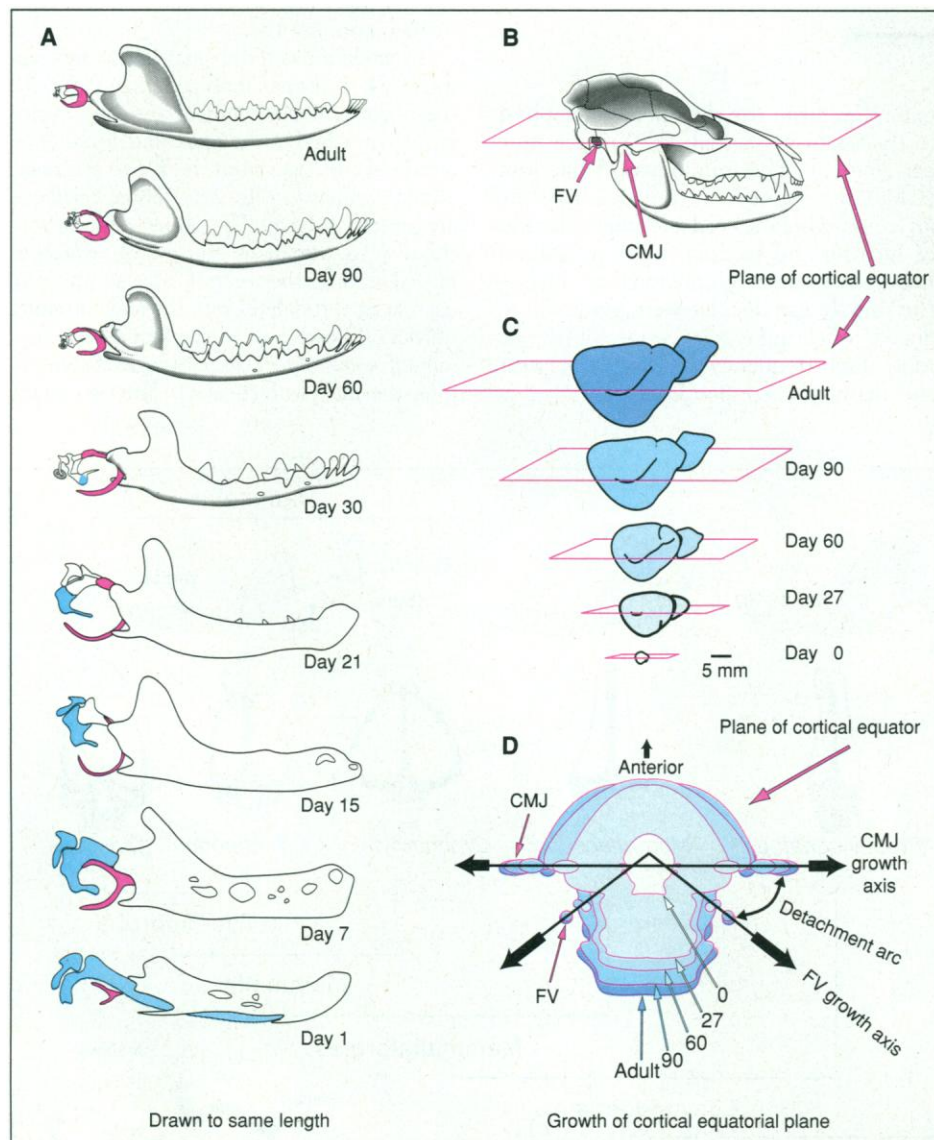


Fig. 2. (A) Development and relative growth of the didelphid mandibular arch, based on cleared and double-stained specimens of *Monodelphis domestica*. Embryonic cartilage is in blue, the tympanic ring or ectotympanic bone is in red, and uncolored regions have become mineralized. Growth of the didelphid forebrain is depicted in (B) through (D), with the cortical equatorial plane shown for reference. (B) Location of cortical equator on didelphid skull. (C) Growth of olfactory bulb and neocortex in right lateral view [after (17)]. (D) Superimposed projections of the cortical equator, from x-ray computed tomographic imaging of *M. domestica*, showing the increase in equatorial circumference with age. Divergent trajectories of the CMJ and FV growth axes define an arc of detachment whose growth leads to detachment and caudal displacement of the auditory chain.

combination of hydrostatic inflation (14) and cell division until 12 weeks after birth (15). As the developing brain balloons upward and backward, it loads and remodels (16) the rear part of the skull.

Developmental cranial remodeling can be

seen in the widening distance between the CMJ and FV as the neocortex equatorial circumference grows. The equatorial segment between the FV and the CMJ defines an arc of detachment (Fig. 2D) for the auditory chain. As the arc's curvature grows, the FV and

attached auditory chain are displaced progressively backward from the CMJ. The geometry of the widening arc describes the detachment of the auditory chain, its path of subsequent displacement, and the timing and extent of relative movement. Detachment of the auditory chain occurs before the onset of auditory functionality. The inner ear is unresponsive to sound until the sixth week after birth and only thereafter does the auditory tract become myelinated (17).

The mammalian neocortex supports heightened olfactory and auditory senses, as well as coincident, overlapping sensory and motor maps of the entire body surface (13, 18). The neocortex is believed to have evolved in relation to the invasion of a nocturnal and arboreal niche (19) and has been implicated in the evolution of endothermy (20). The enlarged cerebellum is related to the acquisition and discrimination of sensory information (21) and to the adaptive coordination of movement through a complex three-dimensional environment (22). Secondary, epigenetic effects (23) accompanied the increased pace and duration of mammalian brain growth involving both the intrinsic organization of the brain and the cranium enclosing it. The repositioning of the middle ear is but one example of a dynamic epigenetic relation between the brain and skull. If this interpretation is correct, an event of fundamental importance in the origin of mammals was a heterochronic perturbation of the brain, inducing it to grow faster for a greater portion of ontogeny, achieving a far larger size than its extinct sister taxa, and triggering a cascade of epigenetic events broadly affecting mammalian life histories.

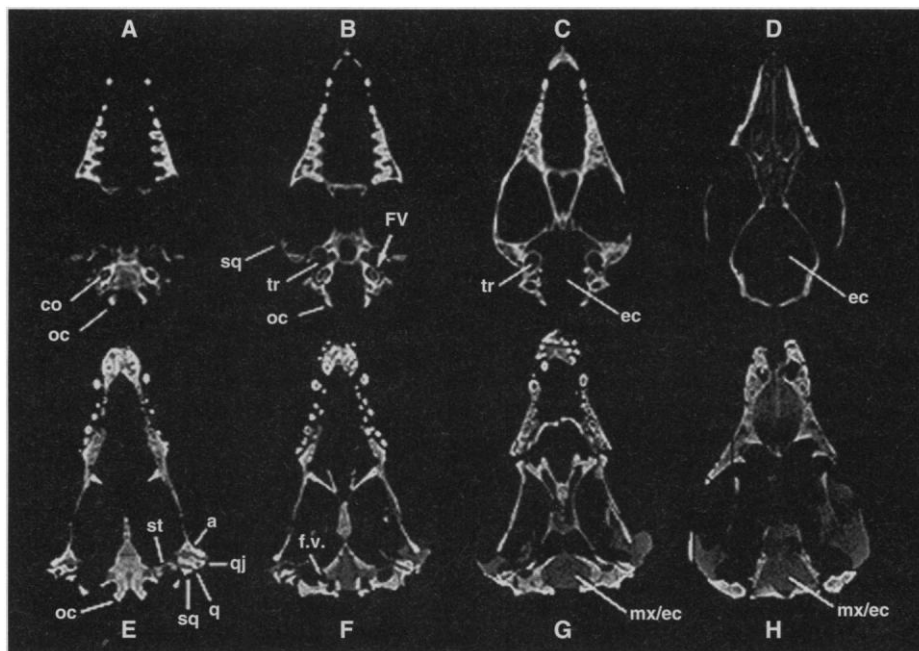


Fig. 3. High-resolution x-ray computed tomographic imagery comparing *Monodelphis* (A through D) (100- μ m slice) and *Thrinaxodon* (E through H) (200- μ m slice). Sections (A) and (E) transect the floor of the braincase; sections (B) and (F) transect the FV; sections (C) and (G) transect the middle of the foramen magnum; and sections (D) and (H) transect the roof of the foramen magnum. Abbreviations: a, articular; co, cochlea; oc, occipital condyle; ec, endocranial cavity; f.v., fenestra vestibuli; mx/ec, matrix in endocranial cavity; q, quadrate; qj, quadratojugal; sq, squamosal; st, stapes; tr, tympanic recess.

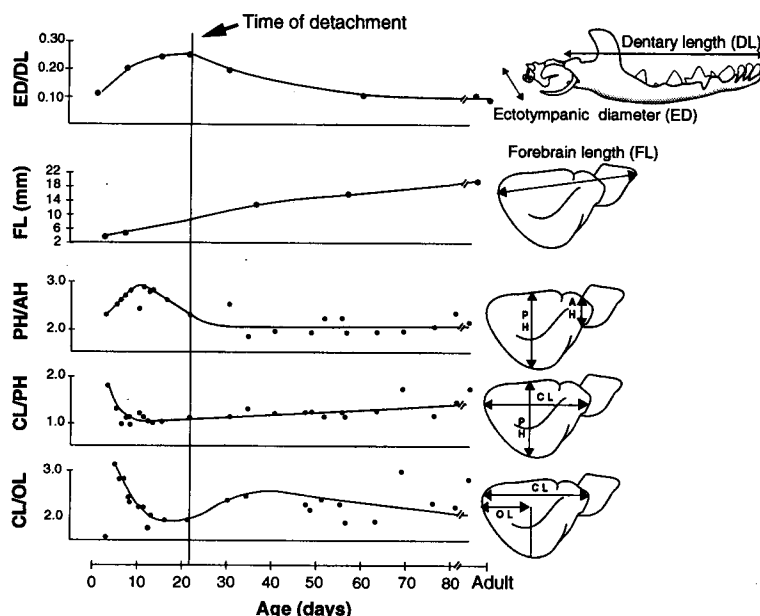


Fig. 4. Differential growth of the didelphid ectotympenic bone and forebrain. In the lower three graphs, relative growth of the forebrain is plotted as a series of ratios defined by the dimensions depicted on the mature forebrain [after (15)]. AH, anterior height; CL, cortical length; OL, occipital length; PH, posterior height.

REFERENCES

1. E. S. Goodrich, *Studies on the Structure and Development of Vertebrates* (Macmillan, London, 1930); G. R. de Beer, *Embryos and Ancestors* (Clarendon, Oxford, 1958).
2. T. Rowe, in *New Perspectives on the History of Life*, M. T. Ghiselin and G. Pinna, Eds. (California Academy of Sciences, San Francisco, in press).
3. E. F. Allin, *J. Morphol.* **147**, 403 (1975); in *The Ecology and Biology of Mammal-Like Reptiles*, N. Hotton III, P. D. MacLean, J. J. Roth, E. C. Roth, Eds. (Smithsonian Institution Press, Washington, DC, 1986), pp. 283-294.
4. D. M. Bramble, *Paleobiology* **4**, 271 (1978); A. W. Crompton and W. L. Hylander, in *The Ecology and Biology of Mammal-Like Reptiles*, N. Hotton III, P. D. MacLean, J. J. Roth, E. C. Roth, Eds. (Smithsonian Institution Press, Washington, DC, 1986), pp. 263-282; A. W. Crompton and P. Parker, *Am. Sci.* **66**, 192 (1978).
5. J. A. Gauthier, A. G. Kluge, T. Rowe, *Cladistics* **4**, 105 (1988); T. Rowe, *J. Vertebr. Paleontol.* **8**, 241 (1988); in *Mammal Phylogeny*, F. S. Szalay, M. J. Novacek, M. C. McKenna, Eds. (Springer-Verlag, New York, 1993), pp. 129-145; _____ and J. A. Gauthier, *Syst. Biol.* **41**, 372 (1992); J. R. Wible, *J. Vertebr. Paleontol.* **11**, 1 (1991).
6. E. C. Olson, *Evolution* **13**, 344 (1959); G. G. Simpson, *ibid.*, p. 405.
7. C. T. Clark and K. K. Smith, *J. Morphol.* **215**, 119 (1993); G. R. de Beer, *The Development of the Ver-*

- tebrate Skull* (Oxford Univ. Press, Oxford, 1937); S. L. Filan, *J. Zool.* **225**, 577 (1991); J. A. McClain, *J. Morphol.* **64**, 211 (1939); E. McCrady Jr., *Am. Anat. Mem. No. 16* (1938); —, E. G. Wever, C. W. Bray, *J. Exp. Zool.* **75**, 503 (1937).
8. S. W. Herring, *Am. Zool.* **33**, 472 (1993); W. Maier, *Gegenbaurs Morphol. Jahrb.* **133**, 123 (1987).
9. T. Rowe, W. D. Carlson, W. W. Bottorff, *Thrinaxodon: Digital Atlas of the Skull* (Univ. of Texas Press, ed. 2, Austin, 1995), available on CD-ROM.
10. P. Alberch, S. J. Gould, G. F. Oster, D. B. Wake, *Paleobiology* **5**, 296 (1979); W. L. Fink, *ibid.* **8**, 254 (1982); A. G. Kluge, in *Ontogeny and Systematics*, C. J. Humphries, Ed. (Columbia Univ. Press, New York, 1988), pp. 57–81; S. J. Gould, *Ontogeny and Phylogeny* (Belknap, Harvard Univ. Press, Cambridge, MA, 1977).
11. G. G. Simpson, *Am. J. Sci.* **214**, 259 (1927).
12. C. Walsh and C. L. Cepko, *Science* **255**, 434 (1992).
13. A. B. Butler, *Brain Res. Rev.* **19**, 66 (1994); R. G. Northcutt, *Am. Zool.* **24**, 710 (1984); P. S. Ulinski, in *The Ecology and Biology of Mammal-Like Reptiles*, N. Hotton III, P. D. MacLean, J. J. Roth, E. C. Roth Eds. (Smithsonian Institution Press, Washington, DC, 1986), pp. 149–171.
14. M. E. Desmond and A. G. Jacobson, *Dev. Biol.* **57**, 188 (1977); R. Jelinek and T. Pexieder, *Folia Morphol.* **17**, 184 (1970); I. C. Nañagas, *J. Philipp. Isl. Med. Assoc.* **5**, 251 (1925); L. H. Weed, *Contrib. Embryol.* **9**, 425 (1920).
15. P. S. Ulinski, *J. Comp. Neurol.* **142**, 33 (1971).
16. D. A. N. Hoyte, *Int. Rev. Gen. Exp. Zool.* **2**, 345 (1966); D. R. Carter, *J. Biomech.* **20**, 1095 (1987); S. A. Newman and W. D. Comper, *Development* **110**, 1 (1990).
17. O. R. Langworthy, *J. Comp. Neurol.* **46**, 201 (1928); O. Larsell, E. McCrady Jr., A. A. Zimmermann, *ibid.* **63**, 95 (1935).
18. R. A. Lende, *Science* **141**, 730 (1963).
19. H. J. Jerison, *Evolution of the Brain and Intelligence* (Academic Press, New York, 1973); in *The Neocortex*, B. L. Findlay et al., Eds. (Plenum, New York, 1990), pp. 5–19; J. Hopson, *Biol. Reptil.* **9**, 39 (1979).
20. J. Allman, *Neuroscience* **2**, 257 (1990).
21. J.-H. Gao et al., *Science* **272**, 545 (1996).
22. W. T. Thatch, H. P. Goodkin, J. G. Keating, *Annu. Rev. Neurosci.* **15**, 403 (1992).
23. B. K. Hall, *Evolutionary Developmental Biology* (Chapman and Hall, London, 1992); J. Hanken and B. K. Hall, Eds., *The Skull*, vols. 1, 2, and 3 (Univ. of Chicago Press, Chicago, IL, 1993).

27 March 1996; accepted 31 May 1996

Demethylation-Induced Developmental Pleiotropy in *Arabidopsis*

Michael J. Ronemus, Massimo Galbiati, Christine Ticknor, Jychian Chen, Stephen L. Dellaporta*

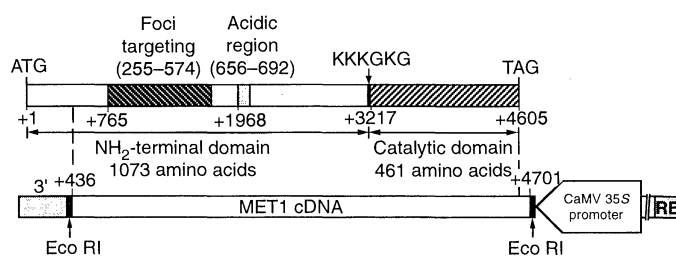
The function of DNA methylation in higher plants was investigated by expression of a complementary DNA encoding a cytosine methyltransferase (MET1) from *Arabidopsis thaliana* as an antisense RNA in transgenic plants. This expression resulted in a 34 to 71 percent reduction in total genomic cytosine methylation. Loss of methylation was observed in both repetitive DNA and single-copy gene sequences. Developmental effects included altered heterochrony, changes in meristem identity and organ number, and female sterility. Cytosine demethylation prolonged both vegetative and reproductive phases of development. These findings implicate DNA methylation in establishing or maintaining epigenetic developmental states in the meristem.

Plant genomes contain relatively large amounts of the modified nucleotide 5-methylcytosine (5mC) (1). Despite evidence implicating cytosine methylation in plant epigenetic phenomena, such as repeat-induced gene silencing (RIGS), cosuppression, and inactivation of transposable elements (2), the role of cytosine methylation in plant developmental processes is not clear. In *Arabidopsis*, *ddm* (decrease in DNA methylation) mutants have been isolated with reduced levels of cytosine methylation in repetitive DNA sequences, although these mutations do not result in any detectable change in DNA methyltransferase enzymatic activity (3, 4). After several generations of self-pollination, *ddm* mutants exhibit a slight delay (1.7 days) in flowering, altered leaf shape, and an increase in cauline leaf number (4).

To address the role of DNA methylation in plant development, we used an antisense strategy to interfere with MET1, a DNA methyltransferase (MTase) gene of *Arabidopsis*, previously cloned by homology to

the mouse gene (Fig. 1) (5, 6). The MET1 gene represents one member of a small gene family in *Arabidopsis* (5) that maps to position 68.9 on chromosome 5, nonallelic to the *ddm1* locus (7). The MET1 gene is expressed in seedling, vegetative, and floral tissues; in the inflorescence, expression is seen at highest levels in meristematic cells by in situ RNA hybridization (8). To inhibit expression of the MET1 gene, we introduced an antisense construct (Fig. 1), consisting of a 4.3-kb MET1 cDNA in the antisense orientation under the control of a constitutive viral promoter (CaMV 35S) (9), into *Arabidopsis* strain Columbia (10) by *Agrobacterium*-mediated transformation

Fig. 1. The predicted MET1 gene product and antisense construct. The predicted gene product of the MET1 locus is a 1534-amino acid protein with a high degree of homology to the mouse MTase, particularly in the catalytic and NH₂-terminal foci targeting domains (5, 30). The MET1 antisense construct is shown below. A 4.3-kb MET1 cDNA spanning the positions indicated was inserted in the reverse orientation with respect to the pMON530 T-DNA vector (9).



(11). In one experiment, a total of nine primary transformants (T0 generation) were recovered; progeny tests indicated that six lines that were further characterized contained single-locus transferred DNA (T-DNA) insertions (12).

Methylation patterns in repetitive DNA sequences were examined by Southern (DNA) hybridization (13). Genomic DNAs were digested with the isochizomers Hpa II or Msp I (Fig. 2, upper panels) and probed with a centromeric repeat or a 5S ribosomal DNA sequence; both repeats are methylated in wild-type genomic DNA (3). Hpa II digestion is inhibited if either cytosine in the CCGG target site is methylated; Msp I can cleave C^{5m}CCGG but not ^{5m}CCGG (14). With both probes, Hpa II digestion revealed a high extent of demethylation in three of six antisense lines (Tr244, 246, and 248: designated “strong”) and in the *ddm1* mutant. Three antisense lines (Tr242, 243, and 245: designated “weak”) showed near wild-type levels of methylation. Msp I digestion was more complete in strong antisense lines than in wild-type or weak antisense lines. These results indicate that strong antisense lines contain substantial demethylation of these repeated sequences at both C^{5m}CCGG and ^{5m}CCGG sites (15).

DNA methylation was examined at four single-copy gene sequences (16) (Fig. 2, lower panels). Substantial demethylation of all four genes was seen only in the strong antisense lines; the *ddm1* mutant showed little

M. J. Ronemus, M. Galbiati, C. Ticknor, S. L. Dellaporta, Department of Biology, Yale University, New Haven, CT 06520-8104, USA.

J. Chen, Academia Sinica, Taipei 11529, Taiwan.

*To whom correspondence should be addressed.